POLITECNICO DI TORINO
Repository ISTITUZIONALE

Vacuum-induced surface freezing for the freeze-drying of the Human Growth Hormone: how does nucleation control affect protein stability?

Original
Vacuum-induced surface freezing for the freeze-drying of the Human Growth Hormone: how does nucleation control affect protein stability? / Oddone, I., Arsiccio, A., Duru, C., Malik, K., Ferguson, J., Pisano, R., Matejtschuk, P.. - In: JOURNAL OF PHARMACEUTICAL SCIENCES. - ISSN 0022-3549. - STAMPA. - 109:1(2020), pp. 254-263. [10.1016/j.xphs.2019.04.014]

Availability:
This version is available at: 11583/2784197 since: 2020-01-22T16:30:36Z

Publisher:
Elsevier B.V.

Published
DOI:10.1016/j.xphs.2019.04.014

Terms of use:

This article is made available under terms and conditions as specified in the corresponding bibliographic description in the repository

Publisher copyright

(Article begins on next page)

16 October 2026

Journal of Pharmaceutical Sciences 109 (2020) 254-263

Contents lists available at ScienceDirect

Journal of Pharmaceutical Sciences

journal homepage: www.jpharmsci.org

Pharmaceutical Biotechnology

Vacuum-Induced Surface Freezing for the Freeze-Drying of the Human Growth Hormone: How Does Nucleation Control Affect Protein Stability?

Irene Oddone [1], Andrea Arsiccio [1], Chinwe Duru [2], Kiran Malik [2], Jackie Ferguson [3], Roberto Pisano [1], Paul Matejtschuk [2,*]

[1] Department of Applied Science and Technology, Politecnico di Torino, 24 corso Duca degli Abruzzi, Torino 10129, Italy
[2] Standardisation Science Section, Analytical and Biological Sciences Division, National Institute for Biological Standards and Control, Blanche Lane, Medicines & Healthcare Products Agency, South Mimms, Potters Bar, Hertfordshire EN6 3QG, UK
[3] Biotherapeutics Division, National Institute for Biological Standards and Control, Medicines & Healthcare Products Agency, Blanche Lane, South Mimms, Potters Bar, Hertfordshire EN6 3QG, UK

ARTICLE INFO

Article history:
Received 31 January 2019
Revised 6 April 2019
Accepted 9 April 2019
Available online 17 April 2019

Keywords:
freeze-drying
nucleation
protein aggregation
protein formulation
HPLC
biopharmaceutical characterization

ABSTRACT

In the present work, the effect of controlled nucleation on the stability of human growth hormone (hGH) during freeze-drying has been investigated. More specifically, the vacuum-induced surface freezing technique has been compared to conventional freezing, both with and without an annealing step. Size exclusion chromatography and cell-based potency assays have been used to characterize the formation of soluble aggregates and the biological activity of hGH, respectively. The results obtained indicate that controlled nucleation has a positive effect on both cycle performance and product homogeneity because of the formation of bigger ice crystals, and characterized by a narrower dimensional distribution. From the point of view of hGH stability, we observed that vacuum-induced surface freezing is not detrimental to the biological activity of the protein, or aggregate formation. In addition, the effect of 2 different formulations, including trehalose or cellobiose, on protein preservation was also considered for this study.

Crown Copyright © 2020 Published by Elsevier Inc. on behalf of the American Pharmacists Association. This is an open access article under the CC BY-NC-ND license (http://creativecommons.org/licenses/by-nc-nd/4.0/).

Introduction

Freeze-drying is the most commonly used method for the preparation of solid protein-based pharmaceuticals. During a freeze-drying cycle, temperature is lowered so as to freeze the product; subsequently, 2 drying steps, called primary and secondary drying, are performed, in which water is removed at low pressure by sublimation or desorption, respectively. The 2 drying phases can be carried out at lower temperature with respect to other drying processes, thus preventing damage to heat-sensitive molecules. In spite of this, the freeze-drying process generates several stresses, which could lead to loss of activity of biopharmaceuticals.[1]

Many of these stresses are linked to the freezing step. Cold denaturation of the protein could arise as a consequence of the low temperature used during freezing,[2] and the active molecule may also adsorb onto and unfold at the ice-water interface.[3] The existence of surface-induced denaturation phenomena is demonstrated by the smaller recovery of protein usually observed at high cooling rates.[3,4] This is due to the smaller dimension, and, therefore, greater surface area to volume ratio, of ice crystals formed at high cooling rates. Another clear evidence of this phenomenon is the decrease in the percentage of unfolded protein molecules observed by increasing the protein concentration in formulations to be frozen, which suggests that protein denaturation is limited by the finite extension of the ice-freeze concentrate interface.[5]

Abbreviations used: C + M, cellobiose + mannitol formulation; DMA, dynamic mechanical analysis; FDM, freeze-drying microscopy; GMP, Good Manufacturing Practice; hGH, human Growth Hormone; HPLC-SEC, high performance liquid size exclusion chromatography; LDH, lactate dehydrogenase; MDSC, modulated differential scanning calorimetry; SEM, scanning electron microscopy; T + M, Trehalose + Mannitol formulation; VIN, vacuum induced nucleation; VISF, vacuum induced surface freezing; XRD, X-ray diffractometry.

* *Correspondence to:* Paul Matejtschuk (Telephone: 0 (+ 44) 1707 641515).
E-mail address: Paul.Matejtschuk@nibsc.org (P. Matejtschuk).

https://doi.org/10.1016/j.xphs.2019.04.014
0022-3549/Crown Copyright © 2020 Published by Elsevier Inc. on behalf of the American Pharmacists Association. This is an open access article under the CC BY-NC-ND license (http://creativecommons.org/licenses/by-nc-nd/4.0/).

Moreover, some components of the formulation could phase separate during freezing, thus providing another interface that could generate surface-induced denaturation.[6] In addition to this, some of the most commonly used buffers, such as the phosphate buffer, could precipitate, leading to a wide pH shift that can denature the protein to a varying degree.[7,8] Finally, cryoconcentration is another possible source of stresses for the biopharmaceuticals to be freeze-dried. The rapid increase in solutes concentration, combined to selective crystallization of formulation components, may lead to significant changes in ionic strength and relative composition of the amorphous phase, possibly destabilizing a protein.[9] As a result of the increased solute concentration, chemical reactions may actually accelerate in a partially frozen aqueous solution.[10] However, it was shown that the critical destabilizing factor is related to adsorption at the ice-freeze concentrate interface.[11] It is therefore clear that a proper control of freezing is of utmost importance because it could lead to improved recovery and increased stability of the therapeutic protein being processed.

An event which strongly affects the outcome of a freezing process is ice nucleation. Nucleation is a stochastic event, and the temperature at which nucleation occurs can vary widely when the traditional freezing techniques are applied, even within the same batch. As the nucleation temperature defines size, number, and morphology of ice crystals, spontaneous nucleation leads to a high intervial variability, causing heterogeneous behavior during drying, as well.[12]

Several methods have thus been proposed to control nucleation. The earliest one was electrofreezing,[13] which uses a high-voltage pulse to generate an ice nucleus on a platinum electrode, that afterward initiates ice crystallization. However, the need for individual electrodes in each sample and, most importantly, the presence of an electrode in direct contact with the product is not practical for good manufacturing practice product manufacture. Subsequently, the ultrasound technique[14-18] was developed, which induces nucleation by an ultrasound transducer. However, this technique, as the electrofreezing one, requires the installation of expensive additional equipment, and this hinders its applicability in manufacturing. A technique that overcomes this limitation is the depressurization method,[19] which involves pressurization at about 3 bar and subsequent depressurization inside the chamber to induce nucleation of ice. This technique is applicable only for freeze driers that are designed to withstand high pressure because equipment-adaptation is very cost-intensive. An alternative method, named ice fog technique, was also proposed,[20,21] in which a flow of cold nitrogen is released within the vacuum chamber, thus generating a suspension of small ice particles. Penetration of this ice fog into the vials induces ice nucleation. This approach is currently available for use in commercial dryers manufactured by IMA Life,[22] while specific optimization is required if the controlled ice nucleation set is being retrofitted to an already existing dryer.

In this study, vacuum-induced nucleation (VIN), or vacuum-induced surface freezing (VISF), was used as previously described by Oddone et al.[23,24] According to this technique, during freezing, the pressure inside the drying chamber is reduced to a low value (~1-2 mbar) for a short time, generally less than 1 min, until nucleation is induced in all vials. This reduction in pressure causes partial evaporation of water and, thus, a fast reduction in product temperature, that promotes the nucleation of ice. With respect to the original approach by Kramer et al.,[25] Oddone et al. proposed the isolation of the drying chamber from the condenser, once the desired value of vacuum is reached. This modification aims to reduce the blow-out phenomena, by letting pressure increase within the freezing chamber during the vacuum period because of water evaporation. The result is that the elegance of the final product is remarkably improved, thus making VISF much more competitive with other controlled freezing strategies. Moreover, an important advantage of the VISF technique is the possibility to precisely control nucleation temperature, without requiring any additional equipment.

Oddone et al.[23,24] showed that VIN can be highly beneficial for homogeneity of the batch and optimization of the freeze-drying cycle. However, the impact of controlled nucleation on the stability of biopharmaceuticals requires further investigation. Geidobler et al.[26] evidenced that controlled ice nucleation may be applied to reduce reconstitution time of highly concentrated lyophilized protein product, and it was reported that it also helped to suppress glass fogging, that is, the undesired migration of protein solutions up on the inner walls of glass vials during the freezing step of lyophilization.[27] Moreover, Fang et al.[28] studied the effect of controlled nucleation on the stability of lactate dehydrogenase (LDH) during both freezing and freeze-drying, but their results were not conclusive. In fact, they found that controlled nucleation remarkably improved LDH recovery after freeze-thawing and also increased batch homogeneity. This result was expected because controlled nucleation results in the formation of larger ice crystals, and, thus, reduced risk of surface-induced denaturation. However, the controlled nucleation technique was not found to be equally advantageous during drying, and a satisfactory explanation for this observation was not provided. In another study,[29] the application of controlled nucleation had neither a positive nor a negative impact on the physicochemical properties and long-term stability of 2 IgG1 antibodies. In the case of high antibody concentration, reduced particle formation was observed in samples frozen with a controlled nucleation approach, but the addition of a surfactant had a much higher stabilizing effect. Therefore, it seems that controlled ice nucleation produced significant benefits on drying duration, product appearance, batch homogeneity, etc., whereas no dramatic improvements were observed for other applications (e.g., small and large molecules).

The objective of this work is, therefore, to provide further insight into the effects of controlled nucleation on protein stability during the freeze-drying process. Moreover, a comparison will be made between trehalose and cellobiose as protein stabilizers, using mannitol as bulking agent. Mannitol is among the most commonly used bulking agents, and trehalose is often selected as lyoprotectant in protein formulations. Cellobiose is not equally common in pharmaceutical formulations, and was used in this work with the aim to evaluate its potential as a protein stabilizer. The high mannitol content should ensure quantitative crystallization during freezing, whereas the protein remains immersed in the amorphous sugar phase. This system is easy to be freeze-dried, and is also representative of the low-density, partially crystalline cakes that are typical of many pharmaceutical products; it represents therefore a suitable model formulation. However, controlled nucleation may be extremely beneficial also for fully amorphous higher-concentrated systems, which are more difficult to process. The application of VISF to amorphous high-concentrated systems will be the subject of future investigations.

For this study, we chose as model protein the human growth hormone (hGH), an aggregation-prone protein widely studied in the literature.[30-36] The extent of protein aggregation after freeze-drying, carried out using either spontaneous or VIN, has been chosen as benchmark to investigate the impact of the selected freezing protocol on protein stability. The impact of the nucleation conditions on the bioactivity of the lyophilized hGH was also assessed by measuring cell proliferation in the lactogenic lymphoblastic rat cell line, Nb2-11.[37] From the results obtained, we will demonstrate that the VISF technique can improve process performance, without having negative effects on protein aggregation or bioactivity.

Table 1
Details of the Freeze-Drying Cycles

	Number of Vials				Freezing Protocol	T_n, °C
	hGH-T + M	hGH-C + M	T + M	C + M		
1	10	10	48	48	Spon.	n. a.
2	10	10	48	48	VISF	−5
3	/	5	/	345	Spon.	n. a.
4	/	5	/	345	VISF	−5
5	/	5	/	345	VISF	−10
6	/	5	/	345	Spon./Anneal.	n. a.
7	21	17	31	31	Spon.	n. a.
8	21	17	31	31	VISF	−5

Materials and Methods

Preparation of Solution

Details of the freeze-drying cycles performed in the present work are reported in Table 1.

For all the cycles, the stability of the hGH was evaluated in the presence of either 6 mg/mL trehalose (T) or 6 mg/mL cellobiose (C). In both cases, mannitol (M), at 42 mg/mL concentration, was used as bulking agent. The objective of this work was to compare 2 freezing protocols (spontaneous and controlled nucleation), and 2 different stabilizers (cellobiose and trehalose), focusing on protein stability. The effect of the freezing protocol should mainly be related to the ice crystal size, and therefore specific surface area, of the cake. The ice crystal size is affected by several factors, encompassing both the freezing protocol (cooling rate, nucleation temperature, presence of an annealing step), and the formulation. The addition of a bulking agent, such as mannitol, as dominant component (42 vs 6 mg/mL) makes it possible to rule out the effect of having a different stabilizer (cellobiose vs. trehalose). Therefore, the ice crystal size should be influenced solely by the freezing protocol. This allows a clearer separation of the contributions of formulation and freezing protocol on protein stability.

All the formulations were prepared in 1.1 mM sodium phosphate buffer, pH 7.8. The hGH used was either the NIBSC standard (WHO International Standard Somatropin, NIBSC code: 98/574) for cycles 3-6, or a commercial time-expired recombinant product supplied by NIBSC (for cycles 1-2 and 7-8), and was dialyzed for about 24 h against the selected formulations using a dialysis kit (Slide-A-Lyzer, 3.5 kDa cutoff; Thermo Fisher Scientific, Hemel Hempstead, UK). Dialysis was carried out under controlled temperature conditions (4°C). At the end of the dialysis, the concentration of hGH was determined by UV spectrophotometry, and the dialyzate was diluted so as to obtain a concentration of hGH of approximately 0.5 mg/mL (cycles 1-6 in Table 1) or 0.25 mg/mL (cycles 7, 8 in Table 1).

Characterization of the Formulations

Modulated differential scanning calorimetry (MDSC), dynamic mechanical analysis (DMA), and freeze-drying microscopy (FDM) analyses were performed on the 2 formulations under investigation.

MDSC was performed using a Q2000 calorimeter (TA Instruments, Elstree, UK). Large volume (100 μL) stainless steel pans were used and 80 μL aliquots were sealed inside them and analyzed against an empty pan as reference. Samples were frozen to −90°C at 10°C/min, and then heated to 25°C at 1.5°C/min, with modulation at 0.23°C/min. Results were analyzed using Universal Analysis software (TA Instruments), and the critical thermal event temperature was assigned based on exotherms in the profiles (at peak maximum). These were detected in reversing, nonreversing, and total heat flow curves with a difference between them of 0.2°C to 0.5°C.

For the dynamic mechanical analyses, a DMA 800 (TA Instruments) was used.[38] A small volume (200 μL, approximately 200 mg) of the solution of interest was pipetted onto one surface of a steel sample tray which was then clamped and inserted into the DMA. Cooling of the system was provided by evaporation of liquid nitrogen. The storage modulus and tan δ values were recorded and plotted against temperature (between −70°C and +10°C), at 1 Hz oscillation frequency. The dynamic amplitude and scan rates were 50 μm and 1°C/min, respectively. The glass transition temperature was determined based on peaks in the tan δ values.

For the FDM analyses, a small amount (5 μL) of each formulation was pipetted onto a special quartz crucible, using a metal shim and coverslip. The crucible was then mounted on a Linkam FDCS196 Cryostage and analyzed using an Olympus BX51 microscope with plane polarized light. Images were captured by a charge-coupled device camcorder. This process was programmed and controlled (Linkam Scientific Ltd., Tadworth, Surrey, UK). Samples were frozen to −50°C at −5°C/min. Subsequently, pressure was lowered to 10 Pa, and the sample was heated at 2°C/min until collapse was observed. The presence of an annealing step at −10°C (for 30 min) was also considered in 2 tests. The system was calibrated using 5% w/v trehalose in water, and single determinations were made for each formulation.

Preparation of Batches

Details on the number of vials within every batch are shown in Table 1. In any case, care was taken to have the active (hGH-containing) vials in the middle of the batch, and therefore shielded by other vials, so as to avoid edge effects. This should guarantee a more homogeneous behavior of active vials in different batches and during different cycles because of a similar exposure to external radiations.

Each vial (5 mL screw capped vial Schott part VC0005 internal diameter 14 mm; Adelphi Healthcare Packaging, Haywards Heath, UK) was filled with 1 mL of solution. In all cases, the excipient formulations were filtered before filling using 0.2 μm filters, whereas the hGH-containing solutions were not filtered, to avoid loss of protein during the process. However, hGH was always added to a prefiltered formulation.

In each batch, the temperature profile inside 3 different vials, containing the placebo formulations, was monitored by means of T-type copper and constantan miniature thermocouples. Thermocouples were placed at the bottom center of the vial, and touching the bottom.

Freeze-Drying Cycles

The freeze-drying cycles were carried out using either the Lyo-Beta 15 (Telstar, Terrassa, Spain), for cycles 1-2, or 25 (Telstar), for cycles 3-6, or the Virtis Genesis 25EL (Biopharma Process Systems, Winchester, Hampshire, UK) freeze-drier, for cycles 7-8. The freezing protocols used in this work were the conventional shelf-ramped freezing (spontaneous nucleation), and the VISF (controlled nucleation). In one case (cycle 6 in Table 1), an annealing step was performed after spontaneous nucleation. The annealing step was performed at −10°C, with a duration of 30 min.

As regards spontaneous freezing, a 0.5°C/min ramp to −45°C was performed. The product was then kept at −45°C for 2 h. By contrast, for VISF, the batch was equilibrated at T_n, as detailed in Table 1, for 1 h. Pressure inside the chamber was then lowered until nucleation was observed (1 mbar). When all the vials nucleated (<1 min), pressure

was quickly released to the atmospheric value. For cycles performed in this work, it took less than 1 min to reach atmospheric pressure. It should be considered that pressure should be released as quickly as possible to avoid boiling of the solution. This result can be achieved by quickly increasing the chamber pressure to a value above the vapor pressure of water at T_n. The subsequent rise to atmospheric value can occur more slowly, without any damage for the product. The product was then kept at −10°C for 1 h. Finally, temperature was decreased to −45°C and held for 2 h.

The 1 h hold at −10°C for the VISF approach is different from an annealing step. In a common annealing step, an already frozen product is brought to higher temperature (above the glass transition) to allow crystallization of formulation components and crystal growth because of Ostwald ripening. By contrast, in the case of the 1 h hold at −10°C for VISF, the product has nucleated already, but is still not completely frozen. The objective, in this case, is to allow a slow growth of the ice crystals, so as to obtain a large ice crystal size. This process occurs slowly, and enough time must be given for the ice crystal growth to complete.

For all the cycles, primary drying was carried out at −35°C and 7 Pa (0.07 mbar) while during secondary drying temperature and pressure were 20°C and 7 Pa, respectively. A 10 h ramp from the primary to secondary drying temperature was used, to reduce the risk of collapse.

During drying, the pressure inside the drying chamber was monitored by means of both a capacitance (MKS Baratron, cycles 1-6) and a thermal conductivity (Pirani, cycles 1-8) manometers. The capacitance manometer always measures the correct value of pressure inside the chamber, whereas the Pirani gauge is calibrated in nitrogen and its readings are therefore shifted to higher values during the primary drying phase, when water vapor is present in the drying chamber as a result of sublimation.

By comparison of the 2 pressure profiles, it is also possible to calculate the onset and offset times.[39] The onset corresponds to the time at which the Pirani gauge reading begins to decay and decline, and indicates that sublimation has ended in a not negligible number of vials. By contrast, at the offset time, the ratio between the capacitance and Pirani readings equals 1, meaning that sublimation has ended in all the vials. The offset marks the end of the primary drying phase, whereas the difference between offset time and onset time (in the following referred to as onset-offset time) is an indicator of within-batch heterogeneity. The larger it is, the more the sublimation behavior of vials within the batch is different.

The ramp to secondary drying was started after the offset time, which can be considered as the end of the sublimation process. By contrast, the duration of secondary drying was, in all cases, set to 5 h.

Residual Moisture Analysis

In the case of cycles 7-8, the residual moisture of dried samples was evaluated using automated Karl Fischer titration. Sample ampoules were opened in a low relative humidity environment using a glove bag (Captair Pyramid, Cole-Parmer, London, UK) flushed with dry nitrogen to an RH level of 5%-10%.

Coulometric Karl Fischer titrations were performed using an automated Karl Fischer system, based on the AquaFast system (A1-Environsciences, Blyth, UK). Samples of lyophilized material were dispensed into septum-sealed autosampler vials in the glove bag environment and then reconstituted remotely with a known aliquot of anolyte. After a period of time to allow insoluble material to settle, an aliquot of the supernatant was titrated into the coulometric Karl Fischer cell. The coulometer was calibrated using the Aquamicron P water standard solution (4 mg/g water content, A-1 Environsciences) and titrations deemed valid only if a 50 μL injection gave a water result of 180-210 μg with a relative standard deviation less than 5% over 3 consecutive titrations. Three placebo-containing vials were analyzed for each formulation, and both the average value and relative standard deviation on the residual moisture could be calculated.

SEM Analysis

In the case of cycles 3-8, the pore dimension of the products obtained after freeze-drying was analyzed using a scanning electron microscope (SEM, FEI type; Quanta Inspect 200, Eindhoven, the Netherlands). The samples were cut along their vertical axis, and 3 SEM images were taken at the top, center, and bottom of the cake.

Afterward, approximately 100 pores were selected in each image, and each of them was approximated to an ellipse. The diameter of the circle having the same area to perimeter ratio of the approximating ellipse was then assumed as pore dimension, and the numerical average (with a corresponding standard deviation) of the obtained distribution was assumed as the average pore size, D_p, of the product.

X-Ray Diffractometry

For cycles 7-8, X-ray diffractometry was also performed on the placebo formulations, to identify the polymorphic state of mannitol in the dried samples. X-ray diffractometry (XRD) patterns were obtained using a PANalytical X'Pert (Cu Kα radiation) diffractometer, within 5°-65° as 2θ range. The data were acquired at each 0.026°. The resulting diffractograms were analyzed using the HighScorePlus program (vers. 3.0.5), by comparison with the X-ray diffraction patterns of the reference materials (α, β, and δ-anhydrous mannitol).

HPLC-SEC Analysis

The soluble aggregates of hGH were measured by size exclusion chromatography (SEC). High-performance liquid size exclusion chromatography (HPLC-SEC) analysis was performed on dried samples, for all the freeze-drying cycles performed. The freeze-dried samples were reconstituted to 1 mL using ultrapure water and then centrifuged for 5 min at 13,000 rpm. A TSKgel G3000 SW_{XL} column (Tosoh Bioscience, Reading, UK) was used on a Thermo Dionex U3000 HPLC system (Thermo Fisher Scientific) using a flow rate of 0.6 mL/min, a run time of 50 min and UV detection at 214 and 280 nm. The mobile phase used was 2-propanol R, 0.063 M phosphate buffer solution pH 7.0 R (3:97 V/V), as suggested in European Pharmacopoeia 9.0.[40] For all batches, 3 hGH-T + M vials, when present, and 3 hGH-C + M vials, were analyzed. For cycles 1-3 and 5-6, 1 hGH-T + M vial, when present, and 1 hGH-C +M vial were analyzed dividing the top part of the cake from the bottom. This was carried out to quantify the degree of intravial heterogeneity in aggregate formation.

Cell Culture

Rat Nb2-11 cells (rat lymphoblast cell line, European Collection of Authenticated Cell Cultures, Public Health England, Salisbury, UK) were routinely grown in suspension culture in Fischer's medium containing 10% (v/v) heat inactivated fetal bovine serum, 10% (v/v) horse serum, 0.075% (v/v) sodium bicarbonate, 50 μM 2-mercaptoethanol, 50 units/mL penicillin, and 0.05 mg/mL streptomycin. Fischer's medium, heat inactivated horse serum and 2-mercaptoethanol were obtained from Thermo Fisher Scientific.

Fetal bovine serum was obtained from BioSera Europe (Nuaille, France) and sodium bicarbonate (7.5%), penicillin, and streptomycin from Sigma Chemical Co., Ltd. (Poole, UK). Cells were maintained by passaging every 4-5 days at a cell density of approximately 1×10^4 cells/mL and incubated at 37°C in an atmosphere of 5% CO_2. At 16-20 h before assay, cells were prepared in culture medium without penicillin and streptomycin at a cell density of 2×10^5 cells/mL and incubated as aforementioned.

Bioassay

The assay is based on the quantitation of ATP in metabolically active cells. The International Standard (WHO International Standard Somatropin, NIBSC code: 98/574) and test samples containing 0.25 mg hGH lyophilized using spontaneous or vacuum-induced nucleation (cycles 7 and 8 in Table 1) with a cellobiose and mannitol excipient (C + M SPON and C + M VIN) or trehalose and mannitol excipient (T + M SPON and T + M VIN) were reconstituted, aliquoted in low-protein binding microfuge tubes (Catalogue number 0030108094, Eppendorf Ltd., Stevenage, UK) and stored at −30°C. Dilutions of the WHO International Standard for Somatropin, 98/574, and test samples were prepared in assay medium that comprised Fischer's medium containing 1% (v/v) horse serum, 0.075% (v/v) sodium bicarbonate, and 50 μM 2-mercaptoethanol. Nb2-11 cells, pretreated as described previously, were washed twice with phosphate buffered saline (pH 7.2), suspended in assay medium at a density of 1×10^5 cells/mL and transferred (50 μL/well) to a 96-well microtitre plate (Greiner Bio-One, Stonehouse, UK, code 655180). Dilutions of standard and test samples were added as an additional 50 μL volume to each well. The maximal cell response was assessed by stimulating with a 10 ng/mL concentration of the International Standard, 98/574. Hormone concentrations are expressed as the final concentration in the wells.

The cells were incubated for 30 ± 2 h in conditions described previously. Proliferation was then estimated by the addition of a 100 μL volume of CellTitre-Glo reagent to each well and incubating with shaking in the dark at room temperature. CellTiter-Glo®Luminescent Cell Viability Assay reagent was obtained from Promega UK (Southampton, UK). The resulting cell extracts were then transferred to a white 96-well plate (Greiner Bio-One code 655075), incubated at room temperature in the dark for 15 min and the luminescence measured using a SpectraMax M5 microplate reader (Molecular Devices (UK) Ltd., Wokingham, UK) controlled by software SoftMax Pro 6 (Version 6.4, 1992-2014 Molecular Devices LLC). Each test dilution was measured in triplicate and test samples were assessed in 2 independent bioassays. Relative bioactivity was assessed by fitting a sigmoidal curve using CombiStats, version 5.0 (1999-2013 EDQM and Council of Europe, Strasbourg, France).

Table 2
Results of MDSC, DMA, and FDM Performed on the 2 Formulations Under Investigation

	T_g', °C (Mid-point)		T_c, °C
	MDSC	DMA	FDM
T + M	−27	−26	−26.5 (collapse)
C + M	−28	−28	−35 (microcollapse), −29 (collapse)
T + M, annealing			−5
C + M, annealing			−7

For the last 2 tests, an annealing step at −10°C was included, and the collapse temperature was measured by FDM.
MDSC, modulated differential scanning calorimetry.

Results

Thermal Characterization of the Formulations

In Table 2, the glass-transition temperature T_g' (mid-point) as measured by MDSC and DMA, and the collapse temperature T_c as measured by FDM are shown. In absence of annealing and with a fast cooling and heating rate, the formulation with the lowest collapse temperature was the cellobiose-based one, which showed a first microcollapse at about −35°C, and complete collapse around −29°C. The collapse temperature observed for the trehalose-based formulation was about 3°C higher (−26.5°C). Results obtained by freeze-drying microscopy are correlated with the glass transition temperature, as measured by both MDSC and DMA. These 2 techniques showed good accordance and revealed a higher critical temperature in the case of trehalose as excipient.

If an annealing step is introduced (T + M, annealing and C + M, annealing in Table 2), or if a slow cooling and heating rate is used, the crystallization of mannitol is promoted. In this case, the formulation is stable also at higher temperatures. The FDM allows identification of the melting temperature of the crystalline phase, which was found to be around −5°C in presence of trehalose, and −7°C in the case of cellobiose as amorphous stabilizer.

If the objective were to optimize the cycle duration, primary drying should be performed at the maximum allowable product temperature which, as illustrated, is a characteristic of the product, and also depends on the presence of an annealing step for crystalline components. A different drying temperature would, however, result in different thermal stresses for the protein. Therefore, as the focus here was on the effect of the freezing protocol on protein stability, primary drying was carried out at the same temperature (−35°C) for all the formulations and freezing protocols under investigation.

Performance of the Freezing Protocols

Previous studies have shown that the use of controlled nucleation, and in particular of the VISF, resulted in a marked reduction of primary drying time.[23,41] This was confirmed by the results obtained in this work. As shown in Table 3, the drying time (difference between the offset of the Pirani decay curve and the initiation of drying) for cycles performed using controlled nucleation was 10%-40% shorter than in the case of conventional freezing. This is due to the higher nucleation temperature in the case of VISF, which leads to the formation of larger pores. In turn, big pores facilitate water vapor diffusion through the dried layer and allow a higher sublimation rate. This is also confirmed by the SEM analysis, Table 4 and Figure 1, which evidenced the presence of larger pores in samples obtained by controlled nucleation. The introduction of an annealing step after spontaneous nucleation, as in cycle 6, increased the pore size and reduced the drying time approximately to the same extent as VISF. This is due to the Ostwald ripening phenomena, which

Table 3
Drying Time (Difference Between the Offset of the Pirani Decay Curve and the Initiation of Drying) and Onset-Offset Times (Difference Between Offset Time and Onset Time) for the Freeze-Drying Cycles Performed

	Freezing Protocol	Drying Time, h	Onset-Offset Time, h
1	Spon.	42	12
2	VISF	27	7
3	Spon.	47	13
4	VISF	35	5
5	VISF	38	4
6	Spon./Anneal.	35	6

Table 4
Pore Dimension D_p in the Dried Product, for the Different Freeze-Drying Cycles Performed

	Freezing Protocol	D_p, μm		
		Bottom	Center	Top
3	Spon.	54 ± 21	80 ± 31	78 ± 27
4	VISF	91 ± 30	169 ± 42	131 ± 41
5	VISF	100 ± 35	110 ± 36	132 ± 36
6	Spon./Anneal.	63 ± 25	77 ± 30	124 ± 32
7-T + M	Spon.	27 ± 14	42 ± 23	33 ± 14
7-C + M	Spon.	21 ± 9	28 ± 12	25 ± 14
8-T + M	VISF	55 ± 23	83 ± 33	57 ± 25
8-C + M	VISF	53 ± 22	81 ± 30	74 ± 33

occur during the annealing step, promoting the dissolution of small crystals and the deposition of the dissolved species on the surfaces of larger crystals.[42] In almost all cases, larger pores were observed at the center of the dried cakes, whereas the smallest pores were at the bottom. This can be explained considering that the larger temperature gradients at the bottom of the product, where the vial is in contact with the drier shelf, and the presence of cryoconcentration effects at the top, promote the formation of smaller ice crystals and therefore smaller pores. Although the average pore size was significantly larger in the case of VISF, the relative standard deviation of the pore dimensions across the height of the cake was similar for all the samples analyzed, and no remarkable difference was observed between spontaneous and controlled nucleation.

The advantages of controlled nucleation were confirmed for cycles 7 and 8, where 2 different formulations, containing either trehalose (T + M) or cellobiose (C + M) were used. In both cases, VISF resulted in a larger ice crystal size, with respect to conventional freezing (Fig. 1).

Figure 2 shows the XRD spectra for the lyophilized samples produced in cycles 7 and 8. The various mannitol polymorphs (α, β, δ) have different stability, with the β form being thermodynamically stable at room temperature, and the other 2 being metastable.[43] In the case of the C + M formulation, both the δ and the β polymorphs were present after both uncontrolled and controlled

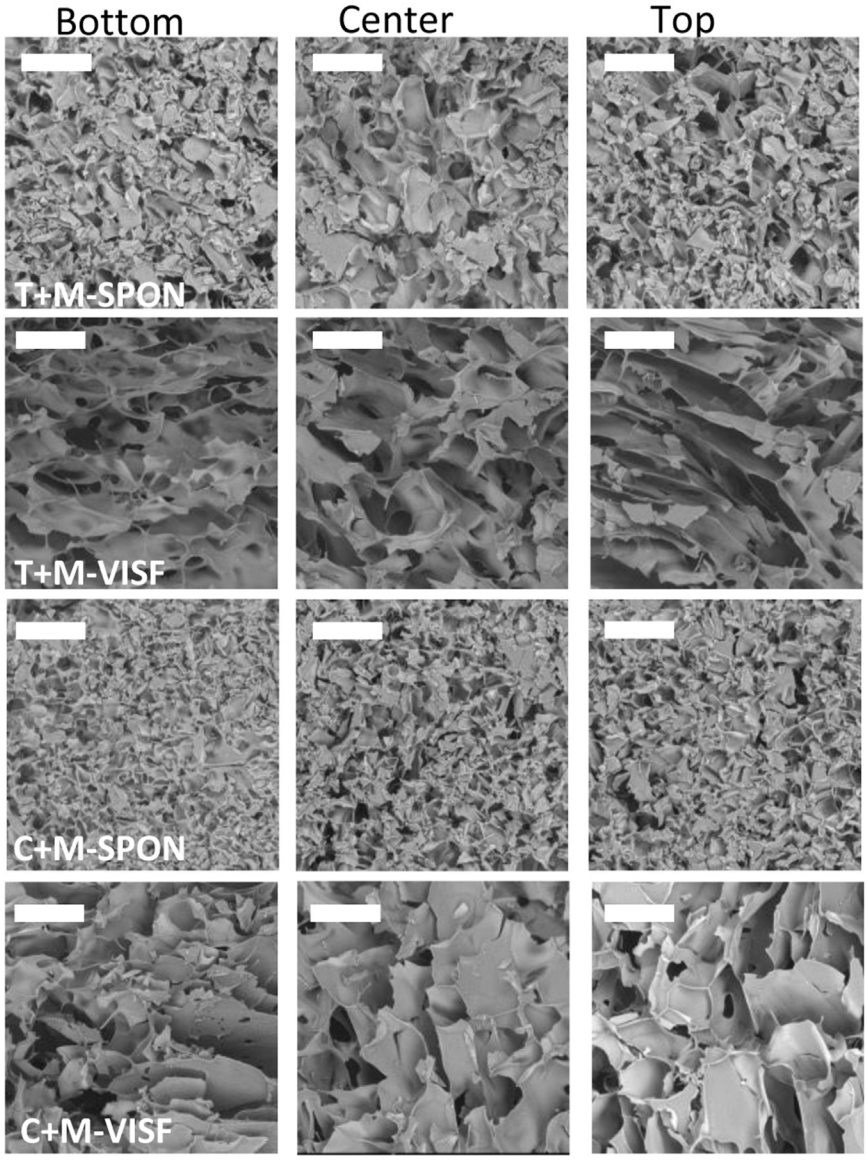

Figure 1. SEM images of the samples obtained at the end of cycles 7 (spontaneous run) and 8 (VISF), for the 2 formulations under investigation (T + M and C + M). The white bar in the figure corresponds to a distance of 200 μm.

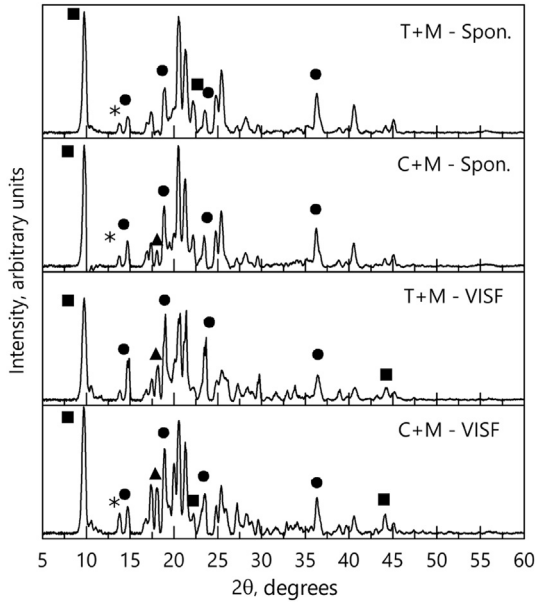

Figure 2. X-ray diffraction spectra for the samples produced in cycles 7 (spontaneous nucleation) and 8 (VISF). The labels identify the most representative peaks for the anhydrous α (*), β (●), and δ (■) polymorphs and for the (▲) hemihydrate.

nucleation. Only traces of α and hemihydrate were present after spontaneous nucleation, whereas the VISF resulted in a slightly higher content of these forms.

Also in the case of the trehalose-based formulation, the β and δ forms were present, whereas the α polymorph was present in traces, and no clear peak for the hemihydrate was detected after spontaneous nucleation. However, the VISF again seemed to slightly increase the presence of α mannitol, and to induce formation of the hemihydrate. This XRD analysis suggests that the controlled nucleation approach may have an impact on the formation of mannitol polymorphs, in line with previous observations.[24,41,44]

Moreover, our results also showed that both controlled nucleation and annealing significantly decreased the onset-offset time (difference between offset time and onset time) with respect to the conventional shelf-ramped freezing (Table 3). Smaller onset-offset times are related to increased uniformity in sublimation behavior within the batch, and therefore reduced intervial variability. The onset-offset time decreased from about 12 or 13 h in the case of spontaneous nucleation (cycles 1 and 3) to 7 h (cycle 2, VISF at $T_n = -5°C$), 5 h (cycle 4, VISF at $T_n = -5°C$), 4 h (cycle 5, VISF at $T_n = -10°C$) or 6 h (cycle 6, where an annealing step was used). This is again in line with previous results.[23,41,42]

Residual Moisture

For the analysis of the residual moisture content, coulometric Karl Fischer titration was performed. The results of this analysis can be found in Table 5.

Table 5
Results of Coulometric Karl Fischer Analysis Performed on Dried Samples, in the Case of Cycles 7-8

	Karl Fischer	
	Water Content w/w ($n = 3$)	CV %
T + M (SPON)	0.49	12.2
C + M (SPON)	0.37	12.6
T + M (VISF)	0.76	25.7
C + M (VISF)	0.53	11.0

What can be observed is that, in the case of both spontaneous and controlled nucleation, the trehalose-based formulation showed a slightly higher residual moisture content after freeze-drying than the cellobiose-based one. Moreover, the VISF always resulted in a higher residual moisture content, with respect to spontaneous nucleation. This is in line with the previous observation that water desorption, during secondary drying, is slower in the case of controlled nucleation.[45]

Soluble Aggregate Formation

In the present work, the formation of soluble aggregates after freeze-thawing (cycles 7-8) or freeze-drying (cycles 1-8) was characterized using HPLC-SEC analysis.

Firstly, a calibration curve for HPLC-SEC was calculated, using a mixture of molecular weight markers ranging from 1350 to 670,000 Da (Bio-Rad's gel filtration standard, BioRad, Watford, UK).

Using this calibration curve, we were able to relate the retention time, as read from the chromatograms, to a corresponding molecular weight. Dimers and higher order soluble aggregates were observed and the relative peak area of these, as a percentage of the total peak area, was used to indicate protein preservation.

As can be observed in Figure 3, HPLC-SEC analysis of available vials suggests that the percentage of high molecular weight species is minimally affected by the use of controlled nucleation. For instance, in cycle 1, which was carried out using conventional freezing, about 3.5% and 5% of aggregates were detected for the T + M and C + M formulations, respectively. When the cycle was repeated using VISF (cycle 2), the percentage of aggregates was about 3% for the trehalose-based formulation and 4.5% for the cellobiose-based one.

To further confirm this behavior, cycles 3-6 were used to investigate the effect of the nucleation temperature, and of annealing as well, in the case of the C + M formulation. The HPLC-SEC results suggest that the aggregation behavior of hGH was not dramatically influenced by changes in these variables. The aggregate content was not significantly affected when the nucleation temperature for the VISF technique was reduced from −5°C to −10°C, or when an annealing step was introduced.

As further analysis, tests 7 and 8 were performed from a previously freeze-thawed solution. As a first step, the protein formulation used for these 2 cycles was quench-frozen to −70°C. After thawing, an aliquot was freeze-dried as described in the Materials

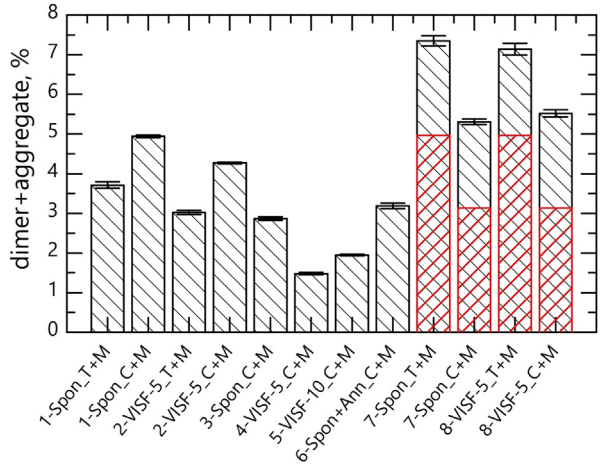

Figure 3. Percentage of dimers and higher order aggregates evidenced by HPLC-SEC after freeze-thawing (red bars) and freeze-drying (black bars). The values for all of the 8 freeze-drying cycles performed, and the 2 formulations under investigation (T + M and C + M), are shown.

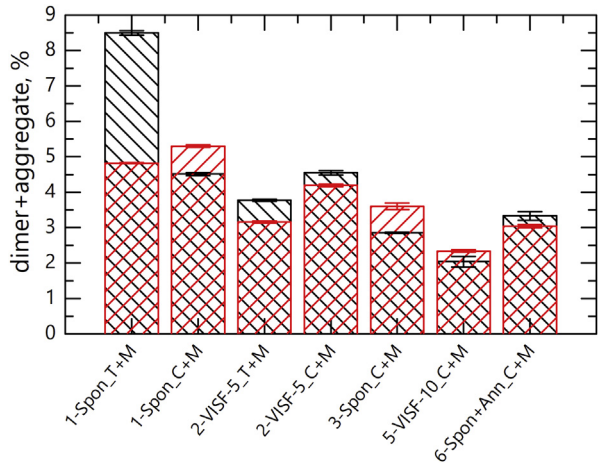

Figure 4. Percentage of dimers and higher order aggregates evidenced by HPLC-SEC in the bottom (red bars) and top (black bars) of freeze-dried samples. The values for cycles 1-3 and 5-6, and for the 2 formulations under investigation (T + M and C + M), are shown.

and Methods section, whereas the remaining part was directly analyzed by HPLC-SEC (red bars in Fig. 3). From this analysis, it seems that most of the aggregates were formed after the freeze-thawing process, especially in the case of the trehalose-based formulation. This may suggest that the hGH should be extremely sensitive to freezing stresses, and in particular to the formation of a large ice-freeze concentrate interface, in line with the experimental observations by Eckhardt et al.[30] However, more freeze-thawing cycles would be needed to draw conclusions on this point.

From the HPLC-SEC results here reported, it seems that no significant difference exists between trehalose and cellobiose as excipients. However, cellobiose is a reducing sugar unlike trehalose, therefore unlikely to be as good in long-term stability at room temperature or above due to Maillard reactions.

Finally, for cycles 1-3 and 5-6, sample vials were analyzed dividing the top part of the cake from the bottom, to quantify the degree of intravial heterogeneity as regards aggregate formation. From Figure 4, it seems that a lower variance across the height of the cake could be observed in the aggregation data collected for samples produced by controlled nucleation. For instance, in the case of conventional freezing, a variance as high as 70% (cycle 1, T + M) was observed, whereas VISF resulted in a variance which was always lower than 20%. Annealing, in the case of cycle 6, improved intravial homogeneity, as well. These results for intravial homogeneity are in line with the onset-offset data reported in Table 3, which are a good indicator of within-batch homogeneity. Overall, these data suggest that controlled nucleation and annealing may improve both intra- and inter-vial homogeneity. However, the HPLC results also suggest that the aggregation behavior of hGH is not dramatically influenced by the use of controlled nucleation.

Comparison of the Bioactivity of Lyophilized hGH Samples

Nb2-11 cells were stimulated with concentrations of hGH ranging from 0.0078 to 1 ng/mL. Maximal fold change, calculated as the ratio of the mean response of the 10 ng/mL positive control ($n = 8$, per plate) to the mean response of the 0 ng/mL control ($n = 8$, per plate), was consistently greater than 2.8. Representative dose response curves for each sample are shown in Figure 5.

All samples were shown to stimulate proliferation of Nb2-11 cells and a sigmoidal (log dose) response was observed. For both formulations, the bioactivity of the vacuum-induced samples was comparable (within 6%) of the bioactivity measured in the spontaneously nucleated samples, thus confirming that VIN does not affect hGH bioactivity as measured in Nb2-11 cells.

Discussion

In the present article, the effect of controlled nucleation, and, more specifically, of the VISF on hGH stability has been investigated. Using cell-based potency assays, we have shown that VISF is not detrimental for the biological activity of hGH. This indicates that the reduction in chamber pressure used to induce nucleation within the vials should not have a negative impact on protein conformational stability. The HPLC analysis also seemed to evidence no significant difference in the aggregation behavior of hGH, no matter which of the 2 freezing protocols was used. What also emerged from our results is that the beneficial effect of the VISF technique on process performance should mainly be related to the formation of bigger ice crystals, and, consequently, of a smaller ice-freeze concentrate interface. The intra- and inter-vial homogeneity was improved by the use of VISF, as well.

These results are in line with the work by Vollrath et al.,[29] where the application of controlled nucleation did not significantly affect the stability of 2 IgG1 antibodies. Our findings compare fairly well also with the report by Fang et al.,[28] where a controlled nucleation approach was found to improve LDH stability after freeze-thawing. However, Fang et al. also observed that the controlled nucleation technique was not equally beneficial for LDH stability during drying. This observation, which remained unanswered in 28, may be related to the different level of residual moisture in samples produced by spontaneous or controlled nucleation. Oddone et al.[24,45] observed that the moisture content during drying was higher in the case of controlled nucleation, because of a lower desorption rate. This is also suggested by the slightly higher residual moisture content detected in this work (Table 5) in samples obtained by VISF. The water content is a crucial parameter for the postdrying stability of proteins, even though a drier cake is not always more stable. For instance, lyophilized BSA and bovine γ-globulin formulations were more stable at 10% water content than at <1%.[46] However, a higher moisture content will result in higher mobility, according to a Williams–Landel–Ferry relation.[47] More specifically, the protein

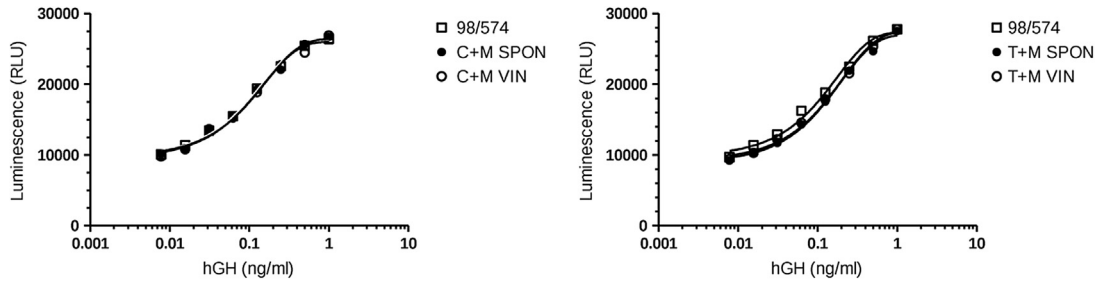

Figure 5. Representative dose-response curves of the stimulation of Nb2-11 cells with hGH. The response to the International standards is shown as open squares (□), spontaneously nucleated samples are shown by closed circles (●), and vacuum-induced nucleated samples by open circles (○).

mobility responsible for both unfolding and aggregation in the dried state is significantly enhanced in the presence of water. The absence of beneficial effects on LDH post-drying stability observed by Fang et al.[28] may therefore be at least partially explained by the higher water content during drying in the case of controlled nucleation.

If this hypothesis were true, the controlled nucleation approach may be beneficial for protein stability in the dried state, provided that a strict control of the moisture level is carried out. This is certainly possible because, on constant processing conditions, the maximum temperature reached during drying in samples produced by VISF is lower than in the case of conventional freezing.[41,45] This means that if process conditions were adjusted so as to have equal product temperature, the rate of water removal could be enhanced during controlled freezing, thus minimizing the detrimental effects related to a high moisture content. Alternatively, a higher temperature could be used during secondary drying in the case of controlled ice nucleation to guarantee postdrying stability. However, further investigation would be required to clarify whether this hypothesis is true.

The thermodynamic mechanism of protein stabilization by preferential exclusion[48] is generally dominant during the first steps of the freezing process, because of the high availability of liquid water before cryoconcentration and drying. However, during primary and secondary drying, protein preservation should be driven by a kinetic mechanism, where the protein motions responsible for unfolding and aggregation are hindered by the formation of a viscous, glassy matrix.[49] A thermodynamic mechanism of protein stabilization in the dried state was also proposed, where the excipient should replace water molecules in hydrogen bonding with the protein, thus inhibiting conformational changes.[50] In the Results section, preliminary results seem to suggest that there may be a difference in the behavior of cellobiose and trehalose during freezing or drying. For instance, the C + M formulation showed only 3% aggregate content after freeze-thawing, whereas in the trehalose-based one, an aggregate concentration as high as 5% was detected. By contrast, the noticeable efficiency of trehalose in the dried state is not surprising because it is well-known that trehalose can form highly structured matrices, characterized by a dense, compact hydrogen-bonding network, which kinetically prevent any protein motion.[51,52] While the data herein presented are not enough to draw conclusions on this point, the theory that not all the excipients are equally effective during freezing and drying has been documented in previous works[50,53] and is supported by *in silico* modeling.[54]

Finally, the XRD analysis suggested that the polymorphs composition of mannitol-based formulations may be influenced by the addition of other excipients, such as trehalose and cellobiose, and by the freezing protocol. This aspect should be taken into account when designing a freeze-drying process for a biopharmaceutical, assuming mannitol as a formulant. Many factors contribute to the specific surface area of a lyophilized cake where mannitol is used as bulking agent. Some of them, such as the ice crystal size and polymorphs composition, are strongly related to the freezing protocol. A second class of factors, such as the surface roughness and crystal habit of the mannitol polymorphs, does not depend on the freezing procedure used. For instance, Cares-Pacheco et al.[55] induced the recrystallization of pure β and δ polymorphs from an aqueous solution of D-mannitol using acetone as an antisolvent. For the α mannitol generation, a crystallization procedure by seeding and fast cooling was used. Afterward, they measured the specific surface area of D-mannitol polymorphs using the IGC-surface energy analyzer (IGC-SEA) from Surface Measurement Systems Ltd. (Wembley, UK), and found that α, β, and δ mannitol have specific surface area of 8.54 m^2g^{-1}, 0.37 m^2g^{-1}, and 1.01 m^2g^{-1}, respectively, indicating that the ice-freeze concentrate surface area, and potentially the protein stability, may be strongly influenced by the polymorphs composition. In a previous work,[24] it was shown that the presence of an annealing step may decrease the amount of δ mannitol in the sample, and promote the formation of the stable β form. The β form should be preferred because, for a proper storage of the active pharmaceutical ingredients, it is desirable that the matrix in which they are immobilized does not significantly modify its properties over time. Moreover, according to the work by Cares-Pacheco et al.,[55] the β form should result in a reduced surface area, and therefore diminished risk of surface denaturation. Finally, as shown by the FDM analyses, primary drying at higher product temperatures would be possible after annealing. For these reasons, an annealing step may therefore prove beneficial.

Conclusions

Our work suggests that VISF is not detrimental for hGH bioactivity, and for its aggregation behavior. These observations, coupled with the positive effect of controlled nucleation on both process performance and product homogeneity, suggest that implementation of a controlled nucleation approach would be beneficial for the freeze-drying process. In this context, a proper formulation should be chosen, as well. The potential benefits of trehalose for kinetic stabilization and cellobiose for thermodynamic prevention of protein unfolding and aggregation during freezing warrant further investigation.

Acknowledgments

The authors would like to acknowledge the technical support of Katherine Partridge. The Italian Ministry of Education, University & Research (MUIR) is acknowledged for the PhD fellowship of Andrea Arsiccio.

References

1. Wang W. Lyophilization and development of solid protein pharmaceuticals. *Int J Pharm*. 2000;203(1-2):1-60.
2. Jaenicke R. Protein structure and function at low temperatures. *Philos Trans R Soc Lond B Biol Sci*. 1990;326(1237):535-551.
3. Strambini GB, Gabellieri E. Proteins in frozen solutions: evidence of ice-induced partial unfolding. *Biophys J*. 1996;70(2):971-976.
4. Chang BS, Kendrick BS, Carpenter JF. Surface-induced denaturation of proteins during freezing and its inhibition by surfactants. *J Pharm Sci*. 1996;85(12):1325-1330.
5. Sarciaux JM, Mansour S, Hageman MJ, Nail SL. Effects of buffer composition and processing conditions on aggregation of bovine IgG during freeze-drying. *J Pharm Sci*. 1999;88(12):1354-1361.
6. Heller MC, Carpenter JF, Randolph TW. Manipulation of lyophilization induced phase separation: implications for pharmaceutical proteins. *Biotechnol Prog*. 1997;13(5):231-238.
7. Gómez G, Pikal MJ, Rodríguez-Hornedo N. Effect of initial buffer composition on pH changes during far-from-equilibrium freezing of sodium phosphate buffer solutions. *Pharm Res*. 2001;18(1):90-97.
8. Murase N, Franks F. Salt precipitation during the freeze-concentration of phosphate buffer solutions. *Biophys Chem*. 1989;34(3):293-300.
9. Al-Hussein A, Gieseler H. The effect of mannitol crystallization in mannitol-sucrose systems on LDH stability during freeze-drying. *J Pharm Sci*. 2012;101(7):2534-2544.
10. Pikal MJ. *Mechanisms of Protein Stabilization during Freeze-Drying Storage: The Relative Importance of Thermodynamic Stabilization and Glassy State Relaxation Dynamics 198-232*. London: Informa Healthcare; 2010.
11. Bhatnagar BS, Pikal MJ, Robin HB. Study of the individual contributions of ice formation and freeze-concentration on isothermal stability of lactate dehydrogenase during freezing. *J Pharm Sci*. 2008;97(2):798-814.
12. Searles JA, Carpenter JF, Randolph TW. The ice nucleation temperature determines the primary drying rate of lyophilization for samples frozen on a temperature-controlled shelf. *J Pharm Sci*. 2001;90(7):860-871.
13. Rau W. Eiskeimbildung durch dielektrische polarisation. *Verlag der Z für Naturforschung*. 1951;6(11):649-657.

14. Inada T, Zhang X, Yabe A, Kozawa Y. Active control of phase change from supercooled water to ice by ultrasonic vibration, Part 1: control of freezing temperature. *Int J Heat Mass Transfer*. 2001;44(23):4523-4531.
15. Zhang X, Inada T, Yabe A, Lu S, Kozawa Y. Active control of phase change from supercooled water to ice by ultrasonic vibration, Part 2: generation of ice slurries and effect of bubble nuclei. *Int J Heat Mass Transfer*. 2001;44(23):4533-4539.
16. Saclier M, Peczalski R, Andrieu J. A theoretical model for ice primary nucleation induced by acoustic cavitation. *Ultrason Sonochem*. 2010;17(1):98-105.
17. Nakagawa K, Hottot A, Vessot S, Andrieu J. Influence of controlled nucleation by ultrasounds on ice morphology of frozen formulations for pharmaceutical proteins freeze-drying. *Chem Eng Process*. 2006;45(9):783-791.
18. Passot S, Trelea IC, Marin M, Galan M, Morris GJ, Fonseca F. Effect of controlled ice nucleation on primary drying stage and protein recovery in vials cooled in a modified freeze-dryer. *J Biomech Eng*. 2009;131(7):074511.
19. Rampersad BM, Sever RR, Hunek B, Gasteyer TH. *Freeze-Dryer and Method of Controlling the Same*. US 824065 B2. U.S. Patent Application Publication; 2012.
20. Patel S, Bhugra C, Pikal M. Reduced pressure ice fog technique for controlled ice nucleation during freeze-drying. *AAPS PharmSciTech*. 2009;10(4):1406-1411.
21. Rambhatla S, Ramot R, Bhugra C, Pikal MJ. Heat and mass transfer scale-up issues during freeze drying, Part 2: control and characterization of the degree of supercooling. *AAPS PharmSciTech*. 2004;5(4):e58.
22. Brower J, Lee R, Wexler E, Finley S, Caldwell M, Studer P. New developments in dontrolled nucleation: commercializing VERISEQ® nucleation technology. In: Varshney D, Singh M, eds. *Lyophilized Biologics and Vaccines*. New York, NY: Springer; 2015.
23. Oddone I, Pisano R, Bullich R, Stewart P. Vacuum-induced nucleation as a method for freeze-drying cycle optimization. *Ind Eng Chem Res*. 2014;53(47):18236-18244.
24. Oddone I, Van Bockstal P-J, De Beer T, Pisano R. Impact of vacuum-induced surface freezing on inter- and intra-vial heterogeneity. *Eur J Pharm Biopharm*. 2016;103:167-178.
25. Kramer M, Sennhenn B, Lee G. Freeze-drying using vacuum-induced surface freezing. *J Pharm Sci*. 2002;91(2):433-443.
26. Geidobler R, Konrad I, Winter G. Can controlled ice nucleation improve freeze-drying of highly-concentrated protein formulations? *J Pharm Sci*. 2013;102(11):3915-3919.
27. Singh SN, Kumar S, Bondar V, et al. Unexplored benefits of controlled ice nucleation: lyophilization of a highly concentrated monoclonal antibody solution. *Int J Pharm*. 2018;552(1):171-179.
28. Fang R, Tanaka K, Mudhivarthi V, Bogner RH, Pikal MJ. Effect of controlled ice nucleation on stability of lactate dehydrogenase during freeze-drying. *J Pharm Sci*. 2018;107(3):824-830.
29. Vollrath I, Friess W, Freitag A, Hawe A, Winter G. Does controlled nucleation impact the properties and stability of lyophilized monoclonal antibody formulations? *Eur J Pharm Biopharm*. 2018;129:134-144.
30. Eckhardt BM, Oeswein JQ, Bewley TA. Effect of freezing on aggregation of human growth hormone. *Pharm Res*. 1991;8(11):1360-1364.
31. Pikal MJ, Dellerman KM, Roy ML, Riggin RM. The effects of formulation variables on the stability of freeze-dried human growth hormone. *Pharm Res*. 1991;8(4):427-436.
32. DeFelippis MR, Kilcomons MA, Lents MP, Youngman KM, Havel HA. Acid stabilization of human growth hormone equilibrium folding intermediates. *Biochim Biophys Acta*. 1995;1247(1):35-45.
33. Costantino HR, Carrasquillo KG, Cordero RA, Mumenthaler M, Hsu CC, Griebenow K. Effect of excipients on the stability and structure of lyophilized recombinant human growth hormone. *J Pharm Sci*. 1998;87(11):1412-1420.
34. Kasimova MR, Milstein SJ, Freire E. The conformational equilibrium of human growth hormone. *J Mol Biol*. 1998;277(2):409-418.
35. Abdul-Fattah AM, Lechuga-Ballesteros D, Kalonia DS, Pikal MJ. The impact of drying method and formulation on the physical properties and stability of methionyl human growth hormone in the amorphous solid state. *Biotechnology*. 2008;97(1):163-184.
36. Salnikova MS, Russell Middaugh CR, Rytting JH. Stability of lyophilized human growth hormone. *Int J Pharm*. 2008;358(1-2):108-113.
37. Tanaka T, Shiu RP, Gout PW, Beer CT, Noble RL, Friesen HG. A new sensitive and specific bioassay for lactogenic hormones: measurement of prolactin and growth hormone in human serum. *J Clin Endocrinol Metab*. 1980;51(5):1058-1063.
38. Gearing J, Malik KP, Matejtschuk P. Use of dynamic mechanical analysis (DMA) to determine critical transition temperatures in frozen biomaterials intended for lyophilization. *Cryobiology*. 2010;61(1):27-32.
39. Patel SM, Takayuki D, Pikal MJ. Determination of end point of primary drying in freeze-drying process control. *AAPS PharmSciTech*. 2010;11(1):73-84.
40. Council of Europe, European Pharmacopoeia Commission. European Pharmacopoeia 9.0. Council of Europe, Strasbourg, France.
41. Arsiccio A, Barresi AA, De Beer T, Oddone I, Van Bockstal P-J, Pisano R. Vacuum induced surface freezing as an effective method for improved inter- and intra-vial product homogeneity. *Eur J Pharm Biopharm*. 2018;128:210-219.
42. Searles JA, Carpenter JF, Randolph TW. Annealing to optimize the primary drying rate, reduce freezing-induced drying rate heterogeneity, and determine T_g' in pharmaceutical lyophilization. *J Pharm Sci*. 2001;90(7):872-887.
43. Burger A, Henck JO, Hetz S, Rollinger JM, Weissnicht AA, Stöttner H. Energy/temperature diagram and compression behavior of the polymorphs of D-mannitol. *J Pharm Sci*. 2000;89(4):457-468.
44. Mehta M, Bhardwaj SP, Suryanarayanan R. Controlling the physical form of mannitol in freeze-dried systems. *Eur J Pharm Biopharm*. 2013;85(2):207-213.
45. Oddone I, Barresi AA, Pisano R. Influence of controlled ice nucleation on the freeze-drying of pharmaceutical products: the secondary drying step. *Int J Pharm*. 2017;524(1-2):134-140.
46. Yoshioka S, Aso Y, Kojima S. Dependence of the molecular mobility and protein stability of freeze-dried γ-globulin formulations on the molecular weight of dextran. *Pharm Res*. 1997;14(6):736-741.
47. Williams ML, Landel RF, Ferry JD. The temperature dependence of relaxation mechanisms in amorphous polymers and other glass-forming liquids. *J Am Chem Soc*. 1995;77(14):3701-3707.
48. Timasheff SN. The control of protein stability and association by weak interactions with water: how do solvents affect these processes? *Annu Rev Biophys Biomol Struct*. 1993;22:67-97.
49. Ohtake S, Kita Y, Arakawa T. Interactions of formulation excipients with proteins in solution and in the dried state. *Adv Drug Deliv Rev*. 2011;63(13):1053-1073.
50. Carpenter JF, Crowe JH, Arakawa T. Comparison of solute-induced protein stabilization in aqueous solution and in frozen and dried state. *J Dairy Sci*. 1990;73(12):3627-3636.
51. Cordone L, Cottone G, Giuffrida S. Role of residual water hydrogen bonding in sugar/water/biomolecule systems: a possible explanation for trehalose peculiarity. *J Phys Condens Matter*. 2007;19(20):205110.
52. Arsiccio A, Pisano R. Water entrapment and structure ordering as protection mechanisms for protein structural preservation. *J Chem Phys*. 2018;148(5):055102.
53. Bhatnagar BS, Bogner RH, Pikal MJ. Protein stability during freezing: separation of stresses and mechanisms of protein stabilization. *Pharm Dev Technol*. 2007;12(5):505-523.
54. Arsiccio A, Pisano R. Clarifying the role of cryo- and lyo-protectants in the biopreservation of proteins. *Phys Chem Chem Phys*. 2018;20(12):8267-8277.
55. Cares-Pacheco MG, Vaca-Medina G, Calvet R, et al. Physicochemical characterization of D-mannitol polymorphs: the challenging surface energy determination by inverse gas chromatography in the infinite dilution region. *Int J Pharm*. 2014;475(1-2):69-81.